

Letter to the editor

Open Access

## Infectivity of SARS-CoV-2 and protection against reinfection in rats

### DEAR EDITOR,

The severe acute respiratory syndrome coronavirus 2 (SARS-CoV-2) pandemic remains an important global public health issue. In this study, we unexpectedly found that wild-type Sprague-Dawley (SD) rats can be infected with the SARS-CoV-2 prototype. Our results showed direct experimental evidence of the infectivity of SARS-CoV-2 infection, subsequent pathogenicity, and protection against reinfection in rats.

Proper animal models for coronavirus disease 19 (COVID-19) are crucial to uncover disease mechanisms and develop appropriate vaccines and drugs. To determine the best model for studying COVID-19, a wide range of animals, including captive and wild animals (deer, lions, and gorillas), companion animals (cats and dogs), farm animals (pigs, chickens, ducks, and mink), and experimental animals (nonhuman primates, mice, hamsters, ferrets, and Chinese tree shrews), have been used to study susceptibility to SARS-CoV-2 infection, with each model harboring its own advantages and disadvantages (Fan et al., 2022; Muñoz-Fontela et al., 2020). Among these COVID-19 models, rhesus macaques well mimic the pathological characteristics of human patients; hamsters are the most suitable for understanding transmission of SARS-CoV-2; and human angiotensin-converting enzyme 2 (*hACE2*) transgenic mice are the most widely used for vaccine and drug evaluation (Fan et al., 2022).

Over the past century, rats have been the preferred rodent model in biomedical research, especially for studies in cardiovascular disease, diabetes, and nutritional metabolic disorders (Modlinska & Pisula, 2020). In the past four decades, mice have become increasingly used in research due to the establishment of mouse embryonic stem cells and gene knockout technology. Nonetheless, rats are still widely

used for toxicological and pharmacological research, including assessment of SARS-CoV-2 vaccines and antiviral drugs (Cao et al., 2022). However, even if good antibody responses to vaccines or potential efficacy of drugs is achieved in rats, other susceptibility models are needed to study the effects of antiviral treatment on SARS-CoV-2 infection (Cohen, 2020). During our SARS-CoV-2 research, we created a *hACE2* transgenic rat model and unexpectedly found that wild-type Sprague-Dawley (SD) rats could be infected with the SARS-CoV-2 prototype. Thus, we designed two experiments to evaluate the susceptibility and subsequent pathogenicity of SARS-CoV-2 infection in rats.

In experiment I, SD rats aged 8–9 weeks were intranasally infected with a  $1 \times 10^5$  median tissue culture infective dose (TCID<sub>50</sub>; 50 µL) of the SARS-CoV-2 prototype (viral sequence available in the China National Microbiology Data Center under Accession No. NMDCN0000HUI) (Figure 1A). Rats were monitored for weight and temperature changes over 16 days (Figure 1B). We observed a gradual increase in body weight in both the infected and mock groups, consistent with the growth characteristics of SD rats at this age, and the increasing trend in body weight continued until the end of the study. However, there was a substantial difference in body weight between the two groups (Figure 1B). Average body temperature was similar in both groups (Supplementary Figure S1), and none of the infected rats exhibited the obvious clinical symptoms of COVID-19 as observed in humans (Wiersinga et al., 2020).

We characterized SARS-CoV-2 replication dynamics in the tracheal and lung tissues of rats. Viral loads were assessed by quantitative real-time polymerase chain reaction (RT-qPCR) of SARS-CoV-2 genomic (nucleoprotein gene (N) and envelope gene (E)) and subgenomic RNAs (sgRNA; subgenomic E (sgE) gene, marker of infectious virus (Dagotto et al., 2021)). Viral genomic RNA (N and E genes) was detected in throat

This is an open-access article distributed under the terms of the Creative Commons Attribution Non-Commercial License (<http://creativecommons.org/licenses/by-nc/4.0/>), which permits unrestricted non-commercial use, distribution, and reproduction in any medium, provided the original work is properly cited.

Copyright ©2022 Editorial Office of Zoological Research, Kunming Institute of Zoology, Chinese Academy of Sciences

Received: 26 September 2022; Accepted: 08 October 2022; Online: 08 October 2022

Foundation items: This study was supported by the National Natural Science Foundation of China (U1902215 to Y.G.Y., 32070569 to L.X.), Applied Basic Research Foundation of Yunnan Province (202001AS070023 to D.Y.), and Key Project of the CAS “Light of West China” Program (to D.Y.)

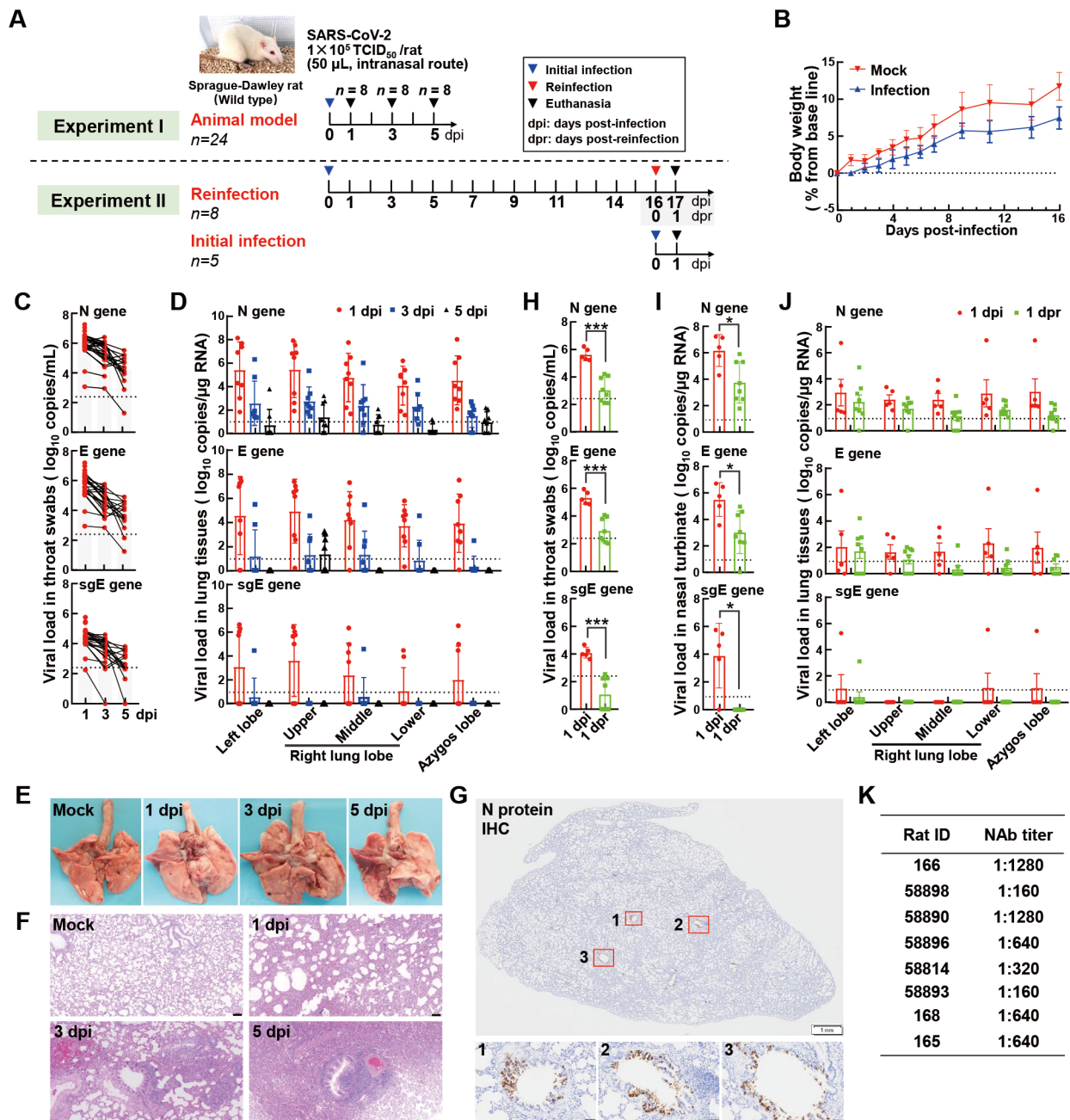


**Figure 1** Infection with SARS-CoV-2 prototype in Sprague-Dawley rats

A: Schematic of infection experiments. B: Alterations in body weight in rats with (infection group) or without (mock group) SARS-CoV-2 infection. Data are mean±standard error of the mean (SEM). C: Viral RNA levels in throat swabs of infected rats at 1 dpi ( $n=32$ ), 3 dpi ( $n=24$ ), and 5 dpi ( $n=16$ ). Each dot indicates log copies of viral genomic N gene (top), E gene (middle), and subgenomic E (sgE) gene (bottom) per swab from an individual rat. D: Viral RNA levels in lungs of infected rats at 1, 3, and 5 dpi. Each red circle (1 dpi,  $n=8$ ), blue square (3 dpi,  $n=8$ ), and black triangle (5 dpi,  $n=8$ ) refers to log viral RNA copies/µg total RNA of lung lobe of an individual rat. E: Gross pathological lung specimens at indicated time points after SARS-CoV-2 infection. F: Hematoxylin/eosin (H&E) staining of the lung sections in SARS-CoV-2-infected rats showing lesions with thickened alveolar septa and infiltration of lymphocytes. Scale bar: 100 µm. G: Immunohistochemical analysis of SARS-CoV-2 N protein in rat lung tissues on 1 dpi. Scale bar: 1 mm for entire lung lobe section (top), 50 µm for enlarged view of boxed areas labeled by numbers in entire section (bottom). H, I: Viral RNA loads in throat swabs (H) and nasal turbinates (I) of rats re-challenged with SARS-CoV-2 for 1 day (1 dpr,  $n=8$ ) were significantly lower than in initial infection group rats (1 dpi,  $n=5$ ). \*:  $P<0.05$ ; \*\*\*:  $P<0.001$ ; two-tailed Student's  $t$ -test. J: Viral RNA levels in lungs of infected rats at 1 dpi (initial infection group) and 1 dpr (reinfection group). K: Neutralizing antibody (NAb) titers in SARS-CoV-2-infected rats for protection against re-challenge. Values in D, H, I, and J are presented as mean±standard deviation (SD). Dotted lines in C and H represent limit of quantification (250 copies/mL). Dotted lines in D, I, and J represent limit of quantification (8.7 copies/µg total RNA of lung).

swabs collected from each infected animal at 1 day and 3 days post-infection (dpi), followed by a sharp decline at 5 dpi, although most infected rats contained viral RNAs at this time (N gene, 15/16; E gene, 14/16; sgE gene, 10/16) (Figure 1C). We detected viral genomic RNA in the lung lobes of infected rats at 1 dpi, and viral sgE gene transcripts reached  $\sim 10^6$  copies/ $\mu\text{g}$  RNA in the lung tissue. For animals euthanized at each time point ( $n=8$ ), six out of eight infected rats at 1 dpi and two out of eight infected rats at 3 dpi had detectable levels of viral sgRNA, but sgRNA was not detected in lung tissue at 5 dpi (Supplementary Figure S2).

To exclude the possibility that the detected sgE transcripts were from residual input inoculum, we measured viral sgRNA levels in the input inoculum for comparison with viral sgRNA levels in the lung tissue of infected rats. Results showed that sgRNA abundance in 50  $\mu\text{L}$  of input inoculum ( $1 \times 10^5$  TCID<sub>50</sub>) was 5.5  $\log_{10}$  copies in total, much lower than the sgRNA level in infected lung tissue (mean viral load of 5.9  $\log_{10}$  copies/ $\mu\text{g}$  total RNA in lung tissue) at 1 dpi. Furthermore, infectious virus was present in the lung tissues of five (TCID<sub>50</sub>/mL value ranges from  $10^{3.8}$  to  $10^{6.8}$ ) out of eight infected rats (Supplementary Figure S3). These results suggested that viral replication can occur at the early stage of SARS-CoV-2 infection in rats.

Gross necropsy revealed visible lung lesions, mainly mild edema and sporadic punctate hemorrhage, in the SARS-CoV-2-infected rats at the three time points (Figure 1E). Histopathological examination of the lung sections from infected animals from 1 dpi to 5 dpi showed pathological indicators of the severity of lung injury, including alveolar septal thickening, interstitial edema, hemorrhage, and mild diffused peribronchial infiltrates (Figure 1F). In addition, immunohistochemical staining of the lung sections detected high expression of the SARS-CoV-2 nucleocapsid (N) protein in the epithelial cells of the bronchioles at 1 dpi (Figure 1G; Supplementary Figure S4). However, N protein staining was not found in the lung sections at 3 dpi and 5 dpi. These results suggested that SARS-CoV-2 can replicate in the upper respiratory tract of rats in the early stages of infection.

In experiment II, we assessed the potential effects of SARS-CoV-2 infection on reinfection. Eight rats were infected with the SARS-CoV-2 prototype ( $1 \times 10^5$  TCID<sub>50</sub>, 50  $\mu\text{L}$ ), then re-challenged with the same amount of SARS-CoV-2 prototype at 16 dpi (reinfection group). Five healthy rats were infected with the SARS-CoV-2 prototype (initial infection group) as a positive control (Figure 1A). Both groups were euthanized one day after infection with SARS-CoV-2. Consistent with the above observations, we detected viral genomic copies and sgRNA in the initial infection group (Figure 1H), with similar viral loads (sgE gene) in throat swabs to those infected animals at 1 dpi in experiment I (Figure 1C). We observed significantly lower levels of viral RNA in throat swabs and nasal turbinate samples from the reinfection group (Figure 1H, 1I). Notably, the sgE transcript was not detected in the nasal turbinate samples from the reinfection group (Figure 1I). Fewer viral genomic copies and sgRNA were found in the lung lobes of the reinfection group compared to the initial infection group (Figure 1J). Only one reinfected rat had detectable (low)

levels of sgE transcript in the left lung lobe, whereas no detectable levels were found in the other seven reinfected rats (Figure 1J). We further measured neutralizing antibody titers in serum samples collected from the reinfected rats. Circulating neutralizing antibodies were detected in all reinfected rats (Figure 1K), indicating an enhanced immune response to SARS-CoV-2 infection. These results suggested that primary exposure to SARS-CoV-2 may have a protective effect against reinfection in rats. It may be worth detecting viral loads at later stages of infection (i.e., 3 days post-reinfection (dpr) and 5 dpr) to assess whether initial SARS-CoV-2 challenge delays viral replication kinetics of reinfection in SD rats.

Here, we provide multiple lines of evidence that the SARS-CoV-2 prototype can infect rats. First, we found high levels of viral genomic copies and sgRNA in throat swabs, nasal turbinate samples, and lung lobe tissues of infected rats at the early stage of infection. Second, we observed viral N protein expression and histopathological changes in the lung sections of infected rats. Third, SARS-CoV-2 infection induced circulating neutralizing antibodies in the rats, which also offered protection against reinfection. However, most infected rats experienced rapid viral clearance, suggesting that SD rats may exhibit a different immune response to SARS-CoV-2 than hamsters and rhesus macaques (Fan et al., 2022; Feng et al., 2022; Muñoz-Fontela et al., 2020).

The conventional view was that wild-type mice could not be infected with SARS-CoV-2 (Muñoz-Fontela et al., 2020). However, with the emergence of SARS-CoV-2 variants of concern, wild-type mice showed an infective and pathogenic phenotype to B.1.1.7 (alpha) and B.1.351 (beta) infection, likely due to mutations of N501Y in the receptor-binding domain (RBD) of the spike (S) protein (Huang et al., 2021). Similarly, wild-type rats could also be infected with the B.1.1.7 and B.1.351 variants (Shuai et al., 2021; Zhang et al., 2022), with those infected with the B.1.351 variant also able to transmit the risk to other rats (Zhang et al., 2022). However, screening samples of Norway rats inhabiting the sewers showed no SARS-CoV-2 infection (Colombo et al., 2022). During our efforts to create a *hACE2* transgenic rat model, we unexpectedly discovered that wild-type SD rats (serving as a control group for *hACE2* transgenic rats) can be infected with the SARS-CoV-2 prototype, thus providing direct evidence of SARS-CoV-2 infection in wild-type SD rats, although the exact reason remains to be explored. Whether other rat strains (particularly wild rats) are susceptible to SARS-CoV-2 infection remains unknown but raises potential ecological risks. Although the binding affinity of the SARS-CoV-2 S protein to rat ACE2 was not higher than that in mice (Cohen, 2020), the expression and distribution of ACE2 in rats may explain the infection. Warnings about hypertension as a moving target in COVID-19 stemmed from studies of pulmonary ACE2 expression in rat models of hypertension (Savoia et al., 2021). In addition, the expression of SARS-CoV-2 cell entry-associated molecules (e.g., furin, TMPRSS2, ADAM17) in rats with heart failure also indicates susceptibility to SARS-CoV-2 (Khoury et al., 2021). Our study not only supports the use of SD rats for assessing the toxicology,

pharmacology, and efficacy of SARS-CoV-2 vaccines and antiviral drugs (Cao et al., 2022), but also for modeling the infection process.

In conclusion, we found that SD rats can be infected with the SARS-CoV-2 prototype, with detectable viral loads in the upper respiratory tract and lung lesions. Initial SARS-CoV-2 infection may provide protection against reinfection.

### SUPPLEMENTARY DATA

Supplementary data to this article can be found online.

### COMPETING INTERESTS

The authors declare that they have no competing interests.

### AUTHORS' CONTRIBUTIONS

D.Y. and Y.G.Y. conceived and designed the study. D.Y., Y.L., L.X., J.B.H., X.L.F., W.Q., and M.H.L. performed the experiments and analyzed the data. J.Xi, J.Xu, L.X.Y., J.L., and Q.C.Z. prepared the animals. D.Y. performed data analyses, D.Y. and Y.G.Y. wrote the manuscript. All authors read and approved the final version of the manuscript.

### ACKNOWLEDGEMENTS

We would like to thank all staff at the Kunming National High-Level Biosafety Research Center for Non-Human Primates for their assistance with the experiments.

Dandan Yu<sup>1,2,3</sup>, Yanghaopeng Long<sup>2</sup>, Ling Xu<sup>1,2,3</sup>,  
Jian-Bao Han<sup>2</sup>, Jiawei Xi<sup>1</sup>, Jianlin Xu<sup>1</sup>, Lu-Xiu Yang<sup>1</sup>,  
Xiao-Li Feng<sup>2</sup>, Qing-Cui Zou<sup>2</sup>, Wang Qu<sup>2</sup>, Jiangwei Lin<sup>1</sup>,  
Ming-Hua Li<sup>2</sup>, Yong-Gang Yao<sup>1,2,3,\*</sup>

<sup>1</sup> Key Laboratory of Animal Models and Human Disease Mechanisms of the Chinese Academy of Sciences, and KIZ-CUHK Joint Laboratory of Bioresources and Molecular Research in Common Diseases, Kunming Institute of Zoology, Chinese Academy of Sciences, Kunming, Yunnan 650201, China

<sup>2</sup> Kunming National High-Level Biosafety Research Center for Non-Human Primates, Center for Biosafety Mega-Science, Kunming Institute of Zoology, Chinese Academy of Sciences, Kunming, Yunnan 650107, China

<sup>3</sup> Kunming College of Life Science, University of Chinese Academy of Sciences, Kunming, Yunnan 650204, China

\*Corresponding author, E-mail: yaoyg@mail.kiz.ac.cn

### REFERENCES

- Cao L, Li YJ, Yang SD, Li GG, Zhou QF, Sun J, et al. 2022. The adenosine analog prodrug ATV006 is orally bioavailable and has preclinical efficacy against parental SARS-CoV-2 and variants. *Science Translational Medicine*, **14**(661): eabm7621.
- Cohen J. 2020. From mice to monkeys, animals studied for coronavirus answers. *Science*, **368**(6488): 221–222.
- Colombo VC, Sluydts V, Mariën J, Vanden Broecke B, Van Houtte N, Leirs W, et al. 2022. SARS-CoV-2 surveillance in Norway rats (*Rattus norvegicus*) from Antwerp sewer system, Belgium. *Transboundary and Emerging Diseases*, **69**(5): 3016–3021.
- Dagotto G, Mercado NB, Martinez DR, Hou YJ, Nkolola JP, Carnahan RH, et al. 2021. Comparison of subgenomic and total RNA in SARS-CoV-2-challenged rhesus macaques. *Journal of Virology*, **95**(8): e02370–20.
- Fan CF, Wu Y, Rui X, Yang YS, Ling C, Liu SS, et al. 2022. Animal models for COVID-19: advances, gaps and perspectives. *Signal Transduction and Targeted Therapy*, **7**(1): 220.
- Feng XL, Yu D, Zhang M, Li X, Zou QC, Ma W, et al. 2022. Characteristics of replication and pathogenicity of SARS-CoV-2 Alpha and Delta isolates. *Virologica Sinica*, <https://doi.org/10.1016/j.virs.2022.09.007>
- Huang HY, Zhu YC, Niu ZB, Zhou LL, Sun Q. 2021. SARS-CoV-2 N501Y variants of concern and their potential transmission by mouse. *Cell Death & Differentiation*, **28**(10): 2840–2842.
- Khoury EE, Knaney Y, Fokra A, Kinaneh S, Azzam Z, Heyman SN, et al. 2021. Pulmonary, cardiac and renal distribution of ACE2, furin, TMPRSS2 and ADAM17 in rats with heart failure: potential implication for COVID-19 disease. *Journal of Cellular and Molecular Medicine*, **25**(8): 3840–3855.
- Modlinska K, Pisula W. 2020. The Norway rat, from an obnoxious pest to a laboratory pet. *eLife*, **9**: e50651.
- Muñoz-Fontela C, Dowling WE, Funnell SGP, Gsell PS, Riveros-Balta AX, Albrecht RA, et al. 2020. Animal models for COVID-19. *Nature*, **586**(7830): 509–515.
- Savoia C, Volpe M, Kreutz R. 2021. Hypertension, a moving target in COVID-19: current views and perspectives. *Circulation Research*, **128**(7): 1062–1079.
- Shuai HP, Chan JFW, Yuen TTT, Yoon C, Hu JC, Wen L, et al. 2021. Emerging SARS-CoV-2 variants expand species tropism to murines. *eBioMedicine*, **73**: 103643.
- Wiersinga WJ, Rhodes A, Cheng AC, Peacock SJ, Prescott HC. 2020. Pathophysiology, transmission, diagnosis, and treatment of coronavirus disease 2019 (COVID-19): a review. *JAMA*, **324**(8): 782–793.
- Zhang C, Cui H, Li ET, Guo ZD, Wang TC, Yan F, et al. 2022. The SARS-CoV-2 B. 1.351 variant can transmit in rats but not in mice. *Frontiers in Immunology*, **13**: 869809.

## **Supplementary Materials**

### **Materials and Methods**

#### **Ethics statement**

All experiments involving live SARS-CoV-2 were conducted in the Animal Biosafety Level 3 (ABSL3) facility at the Kunming Institute of Zoology (KIZ), Chinese Academy of Sciences (CAS). The Institutional Animal Care and Use Committee of KIZ, CAS, approved all protocols used in this study (Approval No: IACUC-RE-2022-04-001).

#### **Virus strain and cells**

The SARS-CoV-2 prototype (viral sequence available in the China National Microbiology Data Center under Accession No. NMDCN0000HUI) was kindly provided by Guangdong Provincial Center for Disease Control and Prevention (Guangdong, China) and has been described in our previous studies (Song et al., 2020; Xu et al., 2020; Zeng et al., 2022). The virus was amplified in Vero-E6 cells. Median tissue culture infective dose (TCID<sub>50</sub>) was used to assess viral infectivity. Virus titers were calculated using the Reed-Muench method (Reed & Muench, 1938).

The Vero-E6 cells were obtained from the Kunming Cell Bank and grown in high-glucose Dulbecco's Modified Eagle Medium (DMEM) supplemented with 10% fetal bovine serum (FBS) and 1% penicillin/streptomycin, and kept in a humidified 5% CO<sub>2</sub> incubator at 37 °C.

#### **Animals and study design**

A total of 41 Sprague-Dawley (SD) rats (four males and 37 females) aged 8–9 weeks were purchased from the Experimental Animal Center of Kunming Medical University. Rats were acclimated to the new environment for a week before SARS-CoV-2 infection. Animals were randomly allocated to different groups for the two experiments. Animals were anesthetized with isoflurane, then intranasally inoculated with 50 µL of SARS-CoV-2 ( $1 \times 10^5$  TCID<sub>50</sub>). All infected animals were housed at the Animal Biosafety Level 3 (ABSL-3) animal core facility of the KIZ on a 12-h light/dark cycle, with free access to food and water.

Experiment I aimed to test whether SD rats could be infected with the SARS-CoV-2 prototype. In brief, 24 rats were infected with SARS-CoV-2 and randomly assigned into three groups (eight animals per group) selected for necropsy at 1 day, 3 days, and 5 days post-infection (dpi), respectively. Nine age-matched rats without treatment were assigned as the control group (mock).

Experiment II aimed to determine whether initial infection provided a protective effect against reinfection with SARS-CoV-2. In brief, we infected eight rats with the same amount of SARS-CoV-2 ( $1 \times 10^5$  TCID<sub>50</sub>) following the same procedures as in Experiment I. We monitored the infected rats for 16 days, after which they received another challenge of SARS-CoV-2 ( $1 \times 10^5$  TCID<sub>50</sub>) following the same procedures (termed reinfection group) as Experiment I, with five rats from the mock group of Experiment I also receiving an infective dose ( $1 \times 10^5$  TCID<sub>50</sub>; termed initial infection

group). Animals in both the reinfection group (1 day post-reinfection (dpr)) and initial infection group (1 dpi) were euthanized for necropsy the day after infection. The remaining four rats in the mock group of Experiment I were used as the non-infected controls for all experiments.

We measured body weight and rectal temperature of all infected rats (32 animals at the beginning of infection) and uninfected rats (nine animals) in both experiments I and II daily at 10:00–11:00 am. We plotted daily changes in average body weight of all animals stratified by infection and non-infection status. The number of infected animals declined from 1 dpi, 3 dpi, and 5 dpi, as eight animals were euthanized for necropsy at each dpi for collecting tissue samples.

Animals were euthanized at indicated time points (Figure 1A) and throat swabs were collected. Each throat swab was placed into 1 mL of DMEM (Thermo Fisher Scientific, USA) and stored at  $-80^{\circ}\text{C}$  until viral load analysis. Gross images of lungs were obtained at time of necropsy. We collected nasal turbinate and lung lobe samples at the indicated time points of necropsy for virological and pathological analyses.

### **Measurement of viral RNAs**

RNA copies per mL of throat swabs or per  $\mu\text{g}$  of lung and nasal turbinate samples were determined by quantitative real-time polymerase chain reaction (RT-qPCR). We extracted total RNA from 200  $\mu\text{L}$  of throat swab solution using a High Pure Viral RNA Kit (Roche, Germany). Extracted RNA was eluted in 50  $\mu\text{L}$  of elution buffer. For lung tissues and nasal turbinate samples, we used Trizol Reagent (Thermo Fisher Scientific, USA) for total RNA isolation from homogenized tissues. Viral RNA copies were detected using a THUNDERBIRD Probe One-Step qRT-PCR kit (TOYOBO, Japan). A 25  $\mu\text{L}$  reaction was established containing 8.7  $\mu\text{L}$  of extracted RNA from throat swabs or 1  $\mu\text{g}$  of total RNA from lung tissues and nasal turbinate samples in a total volume of 8.7  $\mu\text{L}$ , 12.5  $\mu\text{L}$  of 2 $\times$ reaction buffer, 0.625  $\mu\text{L}$  of DNA polymerase, 0.625  $\mu\text{L}$  of RT Enzyme Mix, 0.75  $\mu\text{L}$  of each specific primer (10  $\mu\text{M}$ , Supplementary Table S1), 1  $\mu\text{L}$  of specific probe (5  $\mu\text{M}$ , Supplementary Table S1), and 0.05  $\mu\text{L}$  of 50 $\times$ ROX reference dye. The RT-qPCR was performed using the Applied Biosystems 7500 Real-Time PCR system with the following thermal cycle conditions: 10 min at  $50^{\circ}\text{C}$  for reverse transcription, 60 s at  $95^{\circ}\text{C}$ , followed by 40 cycles of  $95^{\circ}\text{C}$  for 15 s and  $60^{\circ}\text{C}$  for 45 s. In each run, serial dilutions of the SARS-CoV-2 RNA reference standard (National Institute of Metrology, China) were used in parallel to calculate copy numbers in each sample.

### **Viral titers**

Lung tissues from each rat were collected at necropsy and homogenized in 1 mL of serum-free DMEM using a Servicebio Tissue Homogenizer (Wuhan Servicebio Technology Co., Ltd., China). The tissue homogenates were centrifuged at 1 000 g for 10 min at  $4^{\circ}\text{C}$  to pellet cell debris. The homogenate supernatants were serially diluted (10-fold) in serum-free DMEM. Vero-E6 cells ( $2\times 10^4$  cells/well) were grown overnight in a 96-well plate, then 10-fold serial dilutions (100  $\mu\text{L}$ /well) were added to the cultured Vero-E6 cells. After the 96-well plates were incubated at  $37^{\circ}\text{C}$  for 60

min, we added DMEM supplemented with 4% FBS (100  $\mu$ L/well) to the Vero-E6 cells for growth. We monitored the cytopathic effect (CPE) each day, with scoring at 5 dpi. TCID<sub>50</sub> was calculated using the Reed and Muench method (Reed & Muench, 1938).

### **Pathological analysis**

Different lung lobes of rats were fixed in 4% paraformaldehyde for 7 days, processed in paraffin (Leica EG1160), sectioned at a thickness of 3–4  $\mu$ m (Leica RM2255), then stained with hematoxylin and eosin (H&E) followed the procedure described in our previous study (Xu et al., 2020). The slices were imaged using a Nikon Eclipse E100 microscope (Japan) and were blindly evaluated by two pathologists.

Immunohistochemical analysis of lung tissue was performed as described previously (Xu et al., 2020; Zeng et al., 2022). In brief, each section was baked at 65 °C for 30 min, followed by deparaffinization using xylene and subsequent hydration with decreasing concentrations of ethanol (from 100% to 75%). Heat-induced antigen retrieval was performed using sodium citrate buffer (pH 6.0). Endogenous peroxidase was blocked with 3% hydrogen peroxide for 25 min and non-specific binding was blocked with 3% bovine serum albumin (BSA) for 30 min at room temperature. Specimens were incubated overnight at 4 °C with rabbit anti-SARS-CoV-2 nucleocapsid protein antibody (Cell Signaling Technology, Inc., USA, Cat No. #26369, 1:200). The slices were also incubated with rabbit immunoglobulin G (IgG) (Thermo Fisher Scientific, USA, Cat No. #31235) as the negative control for viral antigen staining. Subsequently, the lung slices were incubated with anti-rabbit IgG secondary antibody (Wuhan Servicebio Technology Co., Ltd., China, Cat No. #GB23303) for 50 min at room temperature and visualized with 3,3'-diaminobenzidine tetrahydrochloride (DAB). The slices were counterstained with hematoxylin, dehydrated and mounted on a slide, and viewed under an Olympus OlyVIA microscope (Japan).

### **Neutralizing assay**

Blood samples were collected from rats at necropsy and centrifuged (3 000 g for 10 min at room temperature) to obtain serum samples. After heat inactivation at 56 °C for 30 min, the serum samples were serially diluted in DMEM supplemented with 3% FBS to final dilutions of 1:20, 1:40, 1:80, 1:160, 1:320, 1:640, 1:1 280, and 1:2 560 in a 96-well plate (100  $\mu$ L/well; dilution plate). The virus was diluted in DMEM supplemented with 3% FBS to a final amount of 100 TCID<sub>50</sub> in 100  $\mu$ L of solution. The diluted virus solution (containing 100 TCID<sub>50</sub>) was mixed with each diluted serum sample to form serum-virus mixtures at 37 °C for 60 min.

The Vero-E6 cells ( $2 \times 10^4$  cells/well) were grown overnight in a 96-well plate (culture plate). After removal of culture medium, the serum-virus mixtures (200  $\mu$ L/well) prepared in the dilution plate were transferred to the culture plate, with the cells then grown for 5 days. Plates were monitored daily for CPE. The neutralization titer endpoint was based on inhibition of CPE observed at 5 dpi.

## Statistical analyses

Statistical comparisons were performed using GraphPad Prism v8. Values of body weight were presented as mean±standard error of the mean (SEM) and viral copies were presented as mean±standard deviation (SD). Two-tailed Student's *t*-test was used to compare differences between infected and non-infected groups and  $P<0.05$  was regarded as statistically significant.

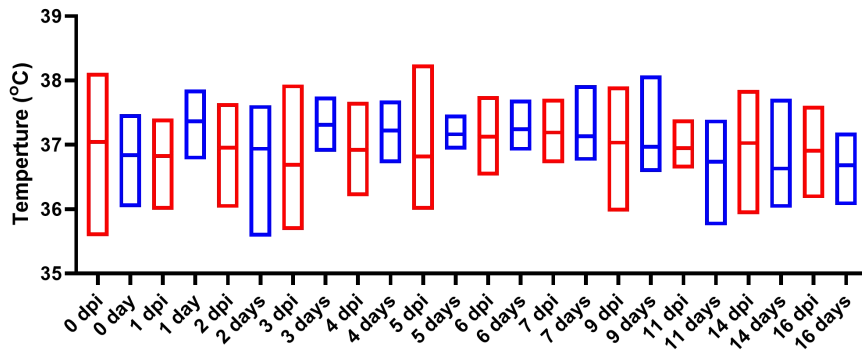
## References

- Reed LJ, Muench H. 1938. A Simple method of estimating fifty per cent endpoints. *American Journal of Epidemiology*, **27**(3): 493–497.
- Song TZ, Zheng HY, Han JB, Jin L, Yang X, Liu FL, et al. 2020. Delayed severe cytokine storm and immune cell infiltration in SARS-CoV-2-infected aged Chinese rhesus macaques. *Zoological Research*, **41**(5): 503–516.
- Xu L, Yu DD, Ma YH, Yao YL, Luo RH, Feng XL, et al. 2020. COVID-19-like symptoms observed in Chinese tree shrews infected with SARS-CoV-2. *Zoological Research*, **41**(5): 517–526.
- Zeng JX, Xie XC, Feng XL, Xu L, Han JB, Yu DD, et al. 2022. Specific inhibition of the NLRP3 inflammasome suppresses immune overactivation and alleviates COVID-19 like pathology in mice. *eBioMedicine*, **75**: 103803.

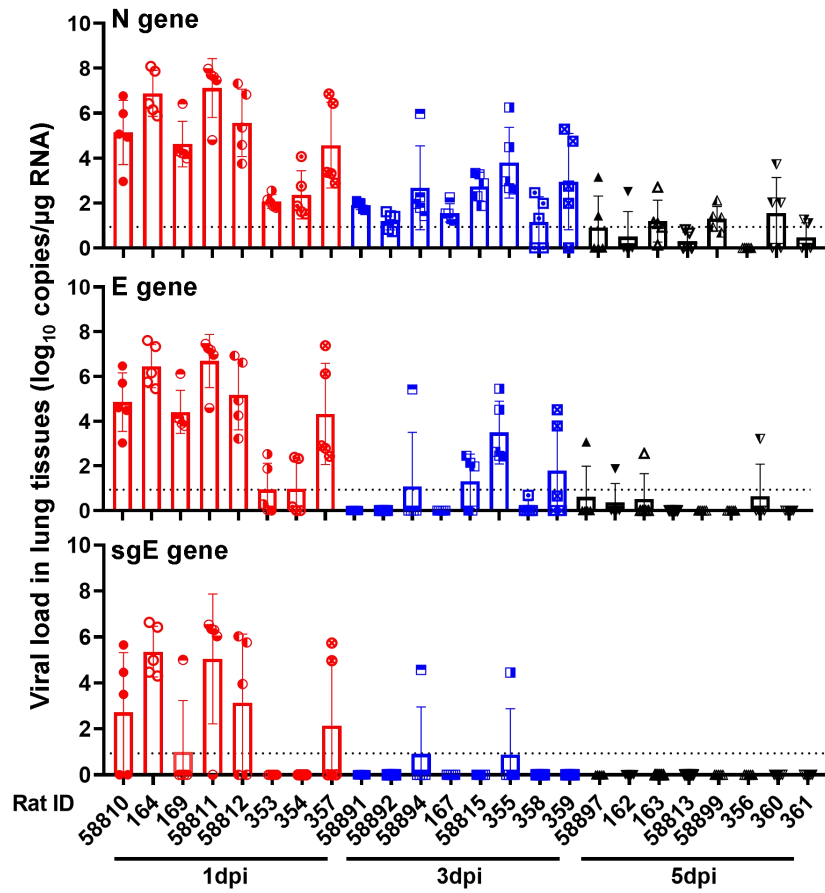
**Supplementary Table S1 Primer pairs and probes for quantification of viral copies**

Primer	Sequence (5'-3')	Target gene
N-F/N-R	5'-GGGGAACCTTCTCCTGCTAGAAT-3' / 5'-CAGACATTTTGCTCTCAAGCTG-3'	genomic N gene
N-P	5'-FAM-TTGCTGCTGCTTGACAGATT-TRMRA-3'	
E-F/E-R	5'-ACAGGTACGTTAATAGTTAATAGCGT-3' / 5'-ATATTGCAGCAGTACGCACACA-3'	genomic E gene
E-P	5'-FAM-ACACTAGCCATCCTTACTGCGCTTCG-TRMRA-3'	
sgE-F/sgE-R	5'-CGATCTCTTGTAGATCTGTTCTC-3' / 5'-ATATTGCAGCAGTACGCACACA-3'	subgenomic E gene (sgE)
sgE-P	5'-FAM-ACACTAGCCATCCTTACTGCGCTTCG-TAMRA-3'	

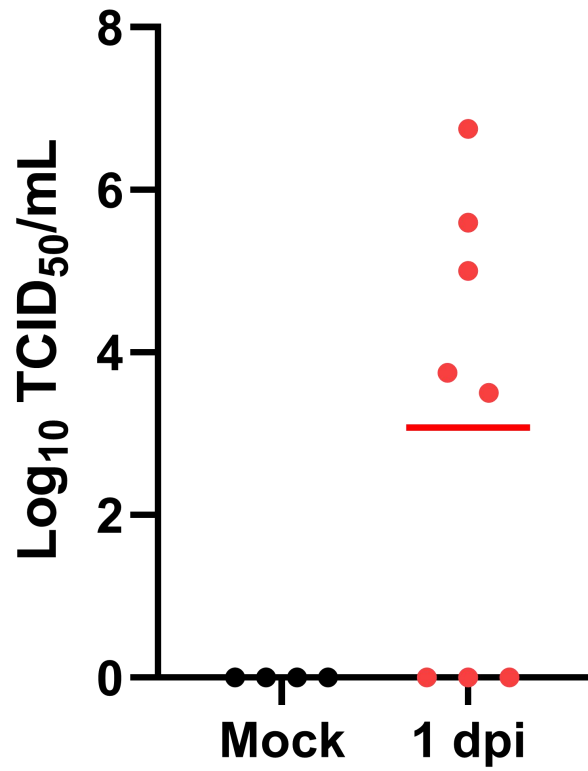
Forward (F) and reverse (R) primers were annotated by adding “-F” and “-R” in each primer name. Probes were annotated by adding “-P” in each probe name. All probes contained 5' fluorescent reporter dye (FAM) and 3' fluorescent quencher (TRMRA).



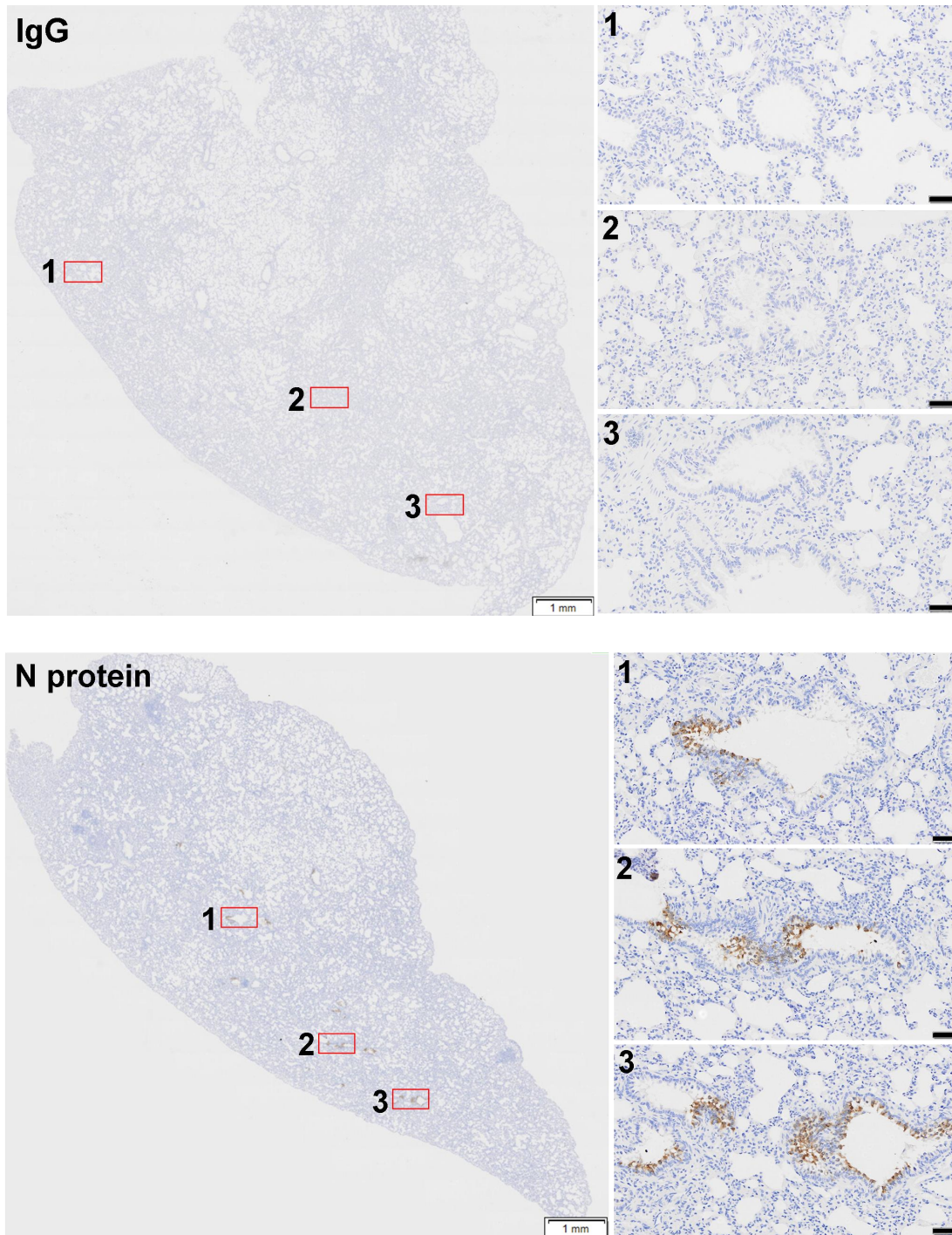
**Supplementary Figure S1** Changes in body temperature over time in SARS-CoV-2-infected rats (infection group, red bars) and uninfected rats (mock group, blue bars). Data are mean±SEM of the infection and mock groups at different days post-infection (dpi).



**Supplementary Figure S2** Viral RNA in five lung lobes of each infected rat at 1 dpi, 3 dpi, and 5 dpi ( $n=8$  rats for each time point). Rat lungs have five lobes. We collected five lung tissue samples from each animal, with one tissue representing one lung lobe. Points in bar refer to viral copy values of five different lung lobes from the same individual. Dotted lines represent limit of quantification (8.7 copies/μg total RNA of lung tissue). Data are mean±SD.



**Supplementary Figure S3** Viral titers in lung tissues of rats in mock group (black circles,  $n=4$ ) and infection group at 1 day post-infection (1 dpi, red circles,  $n=8$ ).



**Supplementary Figure S4** Immunohistochemical analyses showing staining of IgG (negative control; upper) and SARS-CoV-2 N protein (below) in lung tissues of infected rats at 1 dpi. Scale bars, 1 mm for entire lung lobe section and 50 μm for enlarged view of boxed areas labeled by numbers.